The Astronomical Journal, 126:1981–1995, 2003 October

INFRARED SPACE OBSERVATORY AND GROUND-BASED INFRARED OBSERVATIONS OF THE CLASSICAL NOVA V723 CASSIOPEIAE

A. Evans,[1] R. D. Gehrz,[2] T. R. Geballe,[3] C. E. Woodward,[2,4] A. Salama,[5] R. Antolin Sanchez,[5,6] S. G. Starrfield,[7] J. Krautter,[8] M. Barlow,[9] J. E. Lyke,[2] T. L. Hayward,[3] S. P. S. Eyres,[1,10] M. A. Greenhouse,[11] R. M. Hjellming,[12] R. M. Wagner,[13] and D. Pequignot[14]

Received 2003 February 5; accepted 2003 June 19

ABSTRACT

We present observations of the classical nova V723 Cassiopeiae (Nova Cas 1995), obtained both with the *Infrared Space Observatory* (*ISO*) and from the ground. The infrared spectrum was dominated in the first year by H and He recombination lines, and at later times by coronal lines. The H recombination lines imply a reddening of $E(B-V) = 0.78$, an electron temperature of 7000 K, and an electron density of 2×10^8 cm^{-3} on day 250. We argue that the high-ionization species in the infrared are most likely the result of collisional ionization rather than photoionization and are therefore truly "coronal"; we estimate a temperature of 3.2×10^5 K in the coronal region and abundance ratios of S/Si $\simeq$ 2.1, Ca/Si $\simeq$ 1.6, and Al/Si $\simeq$ 1.5. The ejected mass as determined from the Brα line was 2.6×10^{-5} $M_\odot$ for a distance of 4 kpc; however, the mass deduced from the free-free emission, which we conclude arises primarily in the coronal zone, is 4.3×10^{-4} $M_\odot$. V723 Cas did not display the [O IV] 25.89 μm fine-structure line, which was typically seen in the spectra of novae observed with *ISO*. There was no evidence of dust emission in V723 Cas.

Key words: circumstellar matter — novae, cataclysmic variables — stars: individual (Nova Cassiopeia 1995 = V723 Cassiopeiae)

1. INTRODUCTION

Classical nova eruptions occur in semidetached binary systems containing a white dwarf (WD) and a normal companion, usually a main-sequence dwarf. A thermonuclear runaway (TNR) occurs in material that has been accreted onto the surface of the WD. As a result, some 10^{-4} $M_\odot$ of material, enriched in metals as a consequence of the TNR, is ejected at $\sim 10^3$ km s^{-1}. A nova eruption typically goes through an initial optically thick phase, followed by a free-free phase, a nebular phase, and a coronal phase. Some novae also produce dust (which may become optically thick in the optical). Not all novae go through a coronal phase (see Gehrz et al. 1998 for a recent review).

Infrared (IR) observations of classical novae in outburst are now becoming increasingly commonplace (e.g., Gehrz 1988; Bode & Evans 1989; Gehrz 1990; Gehrz et al. 1998 and references therein). IR spectroscopy in particular allows detailed investigation of the dust and coronal development of novae. Observations with the *Infrared Space Observatory* (*ISO*) mission gave us a unique opportunity to follow the evolution of nova eruptions in detail in the far-IR, and there was an active *ISO* target-of-opportunity program to observe novae in eruption; *ISO* observations of novae V705 Cas, V1425 Aql, and CP Cru are reported by Salama et al. (1999) and Lyke et al. (2001, 2003), respectively.

The nova V723 Cas (Nova Cassiopeiae 1995) was discovered on 1995 August 24.5 UT (JD 2,449,954) by Hirosawa & Yamamoto (1995), and spectroscopic confirmation of the nova was given by Iijima & Rosino (1995); premaximum photometry is given by Ohsima, Akazawa, & Ohkura (1996). Further optical spectroscopic observations are described in Iijima, Rosino, & Della Valle (1998), who reported P Cygni absorptions with blueshifts $\sim$150 km s^{-1} relative to the emission. Over the period 63–211 days after outburst, V723 Cas was observed with *IUE*. At this time, the spectrum was dominated by absorption features, indicating the nova was still in its optically thick phase.

IR spectroscopy of V723 Cas in the 0.8–2.5 μm range is given by Rudy et al. (2002), who exploit the low expansion velocities to provide likely identifications (e.g., [Ti VII] 2.205 μm) for a number of previously unidentified lines. IR photometry is given by Munari et al. (1996) and by Kamath & Ashok (1999). Spectropolarimetric observations are described by Johnson, Bjorkman, & Babler (1996), who reported that the polarization was variable, indicating an intrinsic component.

[1] Astrophysics Group, School of Chemistry and Physics, Keele University, Keele, Staffordshire ST5 5BG, UK.
[2] Department of Astronomy, School of Physics and Astronomy, 116 Church Street, SE, University of Minnesota, Minneapolis, MN 55455.
[3] Gemini Observatory, 670 North A'ohoku Place, Hilo, HI 96720.
[4] Visiting Astronomer, Kitt Peak National Observatory, National Optical Astronomy Observatory, which is operated by the Association of Universities for Research in Astronomy, Inc., under cooperative agreement with the National Science Foundation.
[5] *ISO* Data Centre, ESA Satellite Tracking Station, Villafranca del Castillo, Apartado 50727, E-28080 Madrid, Spain.
[6] Instituto de Astronomía y Geodesia (CSIC-UCM), Facultad de CC. Matemáticas, Universidad Complutense, Av. Complutense s/n, E-28040 Madrid, Spain.
[7] Department of Physics and Astronomy, Arizona State University, Tempe, AZ 85287.
[8] Landessternwarte, Königstuhl, D-69117 Heidelberg, Germany.
[9] Department of Physics and Astronomy, University College London, Gower Street, London WC1E 6BT, UK.
[10] Centre for Astrophysics, University of Central Lancashire, Preston PR1 2HE, UK.
[11] NASA Goddard Space Flight Center, Code 685, Greenbelt, MD 20771.
[12] Deceased.
[13] Large Binocular Telescope Observatory, University of Arizona, 933 North Cherry Avenue, Tucson, AZ 85721.
[14] Observatoire de Paris–Meudon, F-92195 Meudon, France.

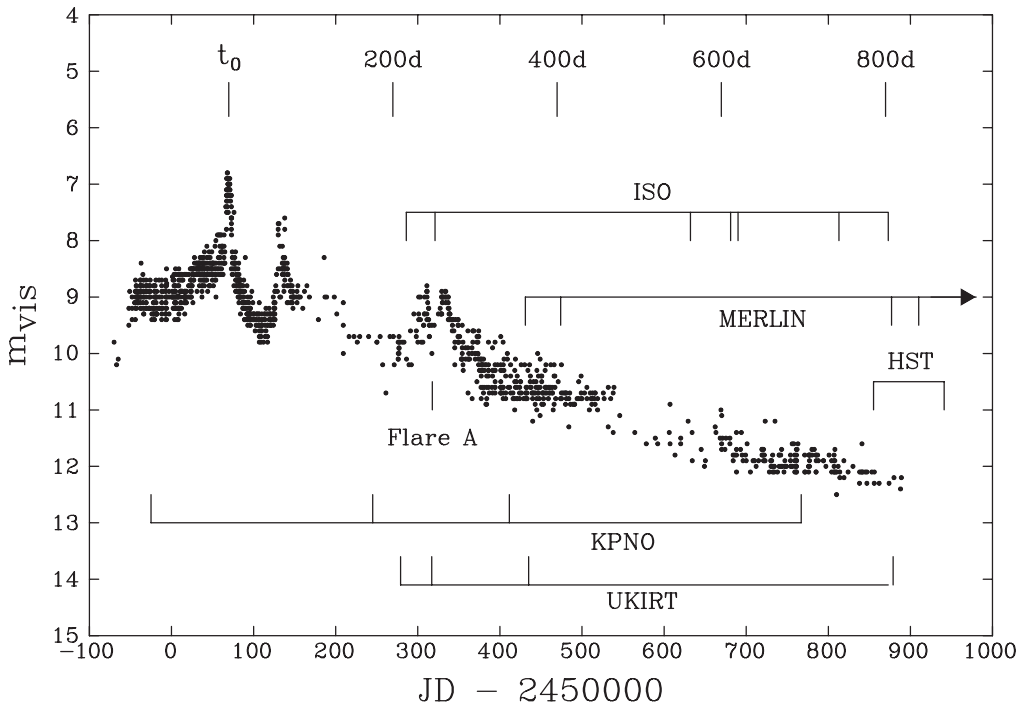

FIG. 1.—Visual light curve of V723 Cas from observations posted on VSNET. Times of *ISO* and ground-based IR (this paper), MERLIN (Heywood et al. 2003), and *HST* (Krautter et al. 2002) observations are shown; note that the MERLIN observations continued beyond JD 2,451,000. Time (in days) from t_0 are given along the top of the diagram.

Eyres et al. (1997) detected V723 Cas at 6 cm on 1996 December 13 and 1997 January 25 (day 520). The nova was not spatially resolved at the time of the earlier observation but was marginally resolved at the second observation. Further radio observations covering the period 1996 February to 2001 October are described by Heywood et al. (2002, 2003), who model the 6 cm light curve using the "Hubble flow" model (e.g., Hjellming et al. 1979).

The visual light curve of V723 Cas (see Fig. 1) is extremely erratic (Munari et al. 1996; Chochol & Pribulla 1997), typical of a "very slow" nova (see Payne-Gaposchkin 1957; Dürbeck 1981; Warner 1989, 1995). Munari et al. (1996) noted a superficial similarity to the visual light curve of the very slow nova HR Del (Nova Del 1967: e.g., Drechsel et al. 1977). They also noted a similarity to the light curve of the "symbiotic nova" PU Vul. Figure 1 indicates that V723 Cas was on the rise for several tens of days after discovery, reaching maximum light around JD 2,450,070 and declining erratically thereafter. Accordingly the time of maximum is not straightforwardly defined; however, we note that there is a sharply defined peak in the light curve around this time. The time of this event is determined to be JD $2{,}450{,}069.7 \pm 0.2$, providing a convenient fiducial for the timescale. We take this as our origin of time, t_0, bearing in mind, however, that the onset of mass ejection will have preceded t_0 by a considerable interval (possibly by as much as $\gtrsim 100$ days).

We note that the light curve of V723 Cas displays several "flarelike" maxima, including a strong flare (hereafter "flare A") in 1996 August, at $t \simeq 250$ days. Such flares may be the result of interaction between ejecta having different velocities or mass transfer bursts from the cool star to the WD (Chochol, O'Brien, & Bode 1999). Similar features are present in the light curve of HR Del. Munari et al. (1996) and Chochol & Pribulla (1997) report large changes ($\Delta\mathrm{mag} \simeq -0.7$) in the $U-B$ color at the time of the peak at t_0.

Chochol et al. (2000) have found the orbital period of the nova system to be 0.69325 ± 0.00018 days. On the basis of relationships between orbital period and properties of the secondary (see Warner 1995 for a summary), the secondary star in V723 Cas must, like the secondary in the GK Per system, be evolved in order for mass transfer to occur. This may have some bearing on the overabundances we tentatively find in the ejecta (see § 7).

V723 Cas was particularly well observed with *ISO*. We present these observations here, together with ground-based IR observations. Many of the *ISO* observations were near-simultaneous with ground-based observations, giving unprecedented IR wavelength coverage over the wavelength range 1–200 μm. Detailed modeling and analysis of the ejected material will be presented elsewhere.

2. OBSERVATIONS

V723 Cas was observed as part of the classical nova target-of-opportunity program on *ISO* (see Table 1, in which TDT is the ISO observation identifier and t is the time in days since t_0). The observations were carried out regularly throughout the *ISO* mission. Ground-based coverage in the near-IR was obtained from the United Kingdom Infrared Telescope (UKIRT), the Kitt Peak National Observatory (KPNO), and from the Wyoming Infrared Observatory (WIRO). A log of ground-based IR observations of V723 Cas is given in Table 2. The *Hubble Space Telescope* (*HST*) and MERLIN (radio) observations are described by Krautter et al. (2002) and by Heywood et al. (2002, 2003),

TABLE 1
ISO Observations of V723 Cas

TDT	Start Time (UT)	JD −2,450,000	*t* (days)	AOT/Speed	Duration[a] (s)
24800901	1996 Jul 22.15	286.7	217.0	SWS-01/4	6538
24800902	1996 Jul 22.23	286.7	217.0	LWS-01/1	1978
24800903	1996 Jul 22.25	286.8	217.0	LWS-01/1	1980
28301904	1996 Aug 26.08	321.6	251.9	SWS-01/4	6538
28301905	1996 Aug 26.15	321.7	252.0	LWS-01/1	1980
59502003	1997 Jul 3.49	633.0	563.3	SWS-01/3	3454
64500309	1997 Aug 21.89	682.4	612.7	SWS-01/3	3454
64500310	1997 Aug 21.93	682.4	612.7	LWS-01/1	1780
65400106	1997 Aug 30.82	691.3	621.6	SWS-01/3	3454
77700106	1997 Dec 31.50	814.0	744.3	SWS-01/3	3454
77700208	1997 Dec 31.54	814.0	744.3	SWS-02	3135
83701909	1998 Mar 1.77	874.3	804.6	SWS-01/3	3454

[a] Observation duration, including instrumental and spacecraft overhead.

respectively; the optical and UV observations will be reported elsewhere.

2.1. *ISO*

The *ISO* observations were obtained using the Short and Long Wavelength Spectrometers (SWS and LWS). The *ISO* spacecraft is described by Kessler et al. (1996). De Graauw et al. (1996) and Clegg et al. (1996) give descriptions of, respectively, the SWS and LWS and their operating modes. Leech et al. (2002)[15] and Gry et al. (2002)[16] give an overview of calibration and aspects of data analysis.

The *ISO* observations generally employed a full grating scan with the SWS using the astronomical observational template (AOT) SWS01 speed 1. However, a number of observations were made using SWS01 speed 3 and 4 and SWS02. We also observed V723 Cas with the LWS using the AOT LWS01; a background LWS observation was carried out at a position 7′ north of the position of the nova. The spectral resolution depends on the wavelength range. Full details may be found in Leech et al. (2002).

The *ISO* data reductions were performed on OLP 10.1 data following the prescriptions described in the Version 3.0 of the Observers SWS Interactive Analysis (OSIA) User Manual. The main tasks consisted of purging the Auto Analysis Result (AAR) and rejecting data points with large error bars. The errors include (1) the accuracy of the dark current determination, (2) the standard deviation of the points in an integration ramp, and (3) the photometric error resulting from a combination of calibration accuracy, photometric check signal determination, and flat-fielding accuracy (see Leech et al. 2002 for details). Occasionally, data from individual detectors or scan directions were rejected if the associated errors were large. The AAR was then sigma-clipped ($\sigma = 3$), flat-fielded, and rebinned to resolution $\lambda/\Delta\lambda = 8000$.

[15] Available at http://www.iso.vilspa.esa.es.
[16] Available at http://www.iso.vilspa.esa.es.

TABLE 2
Ground-Based Observations of V723 Cas

Site	UT Date	JD −2,450,000	*t* (days)	Wavelength Range (Resolution $\Delta\lambda$) (μm)
KPNO	1995 Sep 14.38	−25.1	−94.8	1.15–1.33 (0.0013), 2.01–2.40 (0.0026)
KPNO	1996 Jun 11.44	245.9	176.3	0.89–1.10 (0.00082), 1.06–1.38 (0.0013) 1.40–1.71 (0.0012), 1.52–1.83 (0.0012) 1.93–2.58 (0.0026)
UKIRT	1996 Jul 15	279.5	209.8	1.94–2.09 (0.00062), 2.07–2.23 (0.00062) 2.19–2.53 (0.00125)
UKIRT	1996 Jul 16	280.5	210.8	1.07–1.18 (0.00043), 1.15–1.26 (0.00043) 1.26–1.42 (0.00062)
UKIRT	1996 Aug 22	317.5	247.8	1.07–1.18 (0.00043), 1.15–1.26 (0.00043) 1.26–1.42 (0.00062), 1.94–2.09 (0.00062) 2.07–2.23 (0.00062), 2.19–2.53 (0.00125) 3.25–3.58 (0.0013)
WIRO	1996 Nov 24	411.5	341.8	1.2–4 (0.03–0.1)
UKIRT	1996 Dec 18	435.5	365.8	1.01–1.35 (0.0013), 1.87–2.51 (0.0025) 2.96–3.60 (0.00245)
KPNO	1997 Nov 15.26	767.8	698.1	0.88–1.09 (0.00082), 1.05–1.37 (0.0013) 1.39–1.70 (0.0012), 1.51–1.82 (0.0012) 1.91–2.56 (0.0026)
UKIRT	1998 Mar 7	879.5	809.8	2.94–3.58 (0.0025)

2.2. *Ground-Based Observations*

2.2.1. *UKIRT*

The UKIRT spectra were obtained using the facility cold grating spectrometer, CGS4. The spectrometer employed a 256×256 array of InSb detectors. Pixel scales, spectral coverages, and spectral resolutions varied, but in all cases the lines in V723 Cas were well resolved in the UKIRT spectra. Wavelength calibrations employed observations of arc lamps and are accurate to better than 0.0005 μm. Flux calibration and removal of telluric features were achieved by ratioing near-simultaneously measured spectra of bright dwarf stars with spectral types of A or F at approximately the same air mass as V723 Cas; we interpolated across their absorption lines of atomic hydrogen and used known visible-IR color relations (Tokunaga 2000) to estimate their IR magnitudes.

2.2.2. *KPNO*

Spectra of V723 Cas were also obtained at a variety of epochs on the KPNO 2.1 m telescope using the Cryogenic Imaging Spectrometer (CRSP) with a 256×256 InSb focal plane array (Joyce, Fowler, & Heim 1994) and a $1''.7$ slit. Multiple spectra, using a single grating setting within the bandpass of *IJHK* order sorting filters, were obtained by stepping the source along the slit at $15''$–$20''$ intervals. The photometric standards (HD 18881 in 1995 September, HD 172051 in 1996 June, and HD 18881 in 1997 November) were observed in a similar manner. The two-dimensional spectral images of both the nova and the photometric calibration stars were processed using standard IR techniques (Joyce 1992). Background images used for the first-order removal of the night-sky emission from individual source images were generated by median filtering all images in a given observational set. Individual one-dimensional spectra were subsequently extracted from each image using the IRAF APEXTRACT package. Final spectra were generated by averaging the extracted spectra and scaling each spectrum to the median of the total co-added data set.

Flux calibration of the spectrum was performed by using the spectrum of the photometric standard stars normalized by a blackbody source function appropriate to their spectral type. The blackbody was normalized to the 2.2 μm flux density derived from a Kurucz (1979) model atmosphere. Residual absorption from hydrogen recombination lines in the stellar spectrum were removed by a linear interpolation of the continuum adjacent to the feature prior to division of the object spectrum. Precise wavelength calibration was determined using the strong, unresolved emission lines present in the spectrum of the planetary nebula NGC 7027 observed with the same grating parameters. No atmospheric extinction corrections were applied to the data, since the nova and the comparison photometric standard were observed at similar air masses. The summary of the KPNO 2.1 m (+CRSP) observations are presented in Table 2.

2.2.3. *WIRO*

Low-resolution, near-IR spectroscopy (resolving power of $\lambda/\Delta\lambda \simeq 40$) of V723 Cas was obtained on 1996 November 24.08 UT ($t = 341.8$ days) with the Prism Array Spectrophoto/Polarimeter 2 (Kobayashi et al. 1996) on the WIRO 2.34 m telescope. Measurements were conducted using a $5''$ aperture and a $15''$ east-west nod with a 1 Hz chop rate. The 32 channel Hamamatsu InSb linear array enables simultaneous wavelength coverage from 1.3 to 4.2 μm. The star BS 382 (F0I, $[K] = 3.10$) was used as a photometric standard.

2.3. *Line Fitting*

For the *ISO* data, line fitting was performed within the ISO Spectral Analysis Package (ISAP). We note that the error bars provided by the ISAP line fit task are not representative of the actual uncertainties in the fluxes, full width at half-maximum (FWHM), etc.; we give as the error bar the square root of the quadratic sum of STDEV, GAIN, and RMS, multiplied by the FWHM. Integrated line fluxes and FWHM were determined by fitting one or two (as appropriate) Gaussian profiles after subtracting a linear baseline; the instrumental profile was deconvolved from measured FWHM values. The line fluxes are listed in Table 3. The integrated fluxes and FWHM of the lines in the ground-based data were also determined by fitting Gaussian profiles.

Since we use line ratios to determine physical conditions in the ejecta, etc., we estimate here the effect of various observational uncertainties on the derived parameters. We first note that, within a given atmospheric window, relative errors in the line fluxes range from 2% for the stronger lines to 20% for the weaker. Further, based on uncertainties in the fluxes and effective temperatures of the calibration stars, the flux calibrations for the ground-based data are accurate to $\pm 20\%$. These uncertainties, together with uncertainties in the reddening, propagate through to the uncertainties in the electron temperature T_e and density N_e (§ 4) and abundances (§ 7).

Our assumed uncertainty in the reddening (§ 4.2) results in relative errors in the fluxes of $\pm 8\%$ at 1 μm, and $\pm 2\%$ at 4 μm. Our determination of N_e and T_e employs flux ratios formed from lines close in wavelength and therefore within an atmospheric window and unaffected by uncertainties in reddening; the uncertainties in the flux ratios are therefore dominated by those in the line fits. The formal error in the flux ratio is therefore $\sim 15\%$ at most, which is somewhat less than the scatter ($\sim 25\%$) in the possible values of N_e and T_e.

TABLE 3
LINE FLUXES FROM *ISO* DATA

t (days)	λ_{obs} (μm)	ID	V (km s^{-1})	Flux (10^{-16} W m^{-2})
563.3	2.904	[Al V]	324	24 ± 1.0
	3.091	He II 7–6	346	9 ± 0.9
	3.205	[Ca IV]	325	7 ± 0.8
612.7	2.902	[Al V]	...	<16
	3.206	[Ca IV]	326	12 ± 2.6
621.6	2.904	[Al V]	402	22 ± 1.1
	3.091	He II 7–6	285	7 ± 0.7
	3.205	[Ca IV]	523	18 ± 1.0
744.3	2.903	[Al V]	395	21.4 ± 5.8
	3.091	He II 7–6	286	6.1 ± 2.7
	3.206	[Ca IV]	291	9.8 ± 2.9
744.3	2.904	[Al V]	304	19.9 ± 4.3
	3.091	He II 7–6	263	7.1 ± 1.1
	3.207[a]	[Ca IV]	273	9.9 ± 0.9
804.6	2.903	[Al V]	338	40 ± 1.2
	3.205	[Ca IV]	263	8 ± 0.7
	3.661	[Al VI]	523	12 ± 1.3

[a] Double peaked.

Further, in view of the uncertainty in the flux calibration, flux ratios formed from lines in different atmospheric windows have uncertainty in the range 20% (strong lines) to 30% (weak lines), resulting in similar uncertainties in the abundance ratios.

3. EMISSION-LINE SPECTRUM

The evolution of a selected part of the spectral coverage obtained with the *ISO* SWS (2.38–4.08 μm) is shown in Figure 2. The continuum is negligible, but we clearly detect several H recombination lines and He II 7–6. In addition, there are several strong coronal lines, particularly [Al V] and [Ca IV].

The ground-based spectra from UKIRT and KPNO are shown in Figures 3–7. The IR spectrum for the $\sim$900 days of our observations (i.e., $t \simeq -95$ to $t \simeq 800$ days) was dominated by H I and He II recombination lines, together with coronal emission. The observed fluxes in a number of H recombination lines are given in Table 4.

There are some lines in the *K*-band spectrum of V723 Cas that were also present (but unidentified) in the IR spectrum of the slow nova PW Vul (Williams, Longmore, & Geballe 1996). These include $\lambda = 1.957$, 1.975, 1.987, 2.001, and 2.088 μm (see Figs. 6 and 8). A likely identification for these lines is Fe II, at 1.9577 μm ($z^4F^\circ_{5/2} - c^4F_{7/2}$), 1.9752 μm ($z^4F^\circ_{5/2} - c^4F_{5/2}$), 1.9874 μm ($z^4D^\circ_{3/2} - c^4F_{3/2}$), 2.0016 μm ($z^4F^\circ_{5/2} - c^4F_{3/2}$), and 2.0894 μm ($z^4F^\circ_{3/2} - c^4F_{3/2}$) (see Rudy et al. 2003, and in preparation). The line at 2.015 μm, however, remains unidentified.

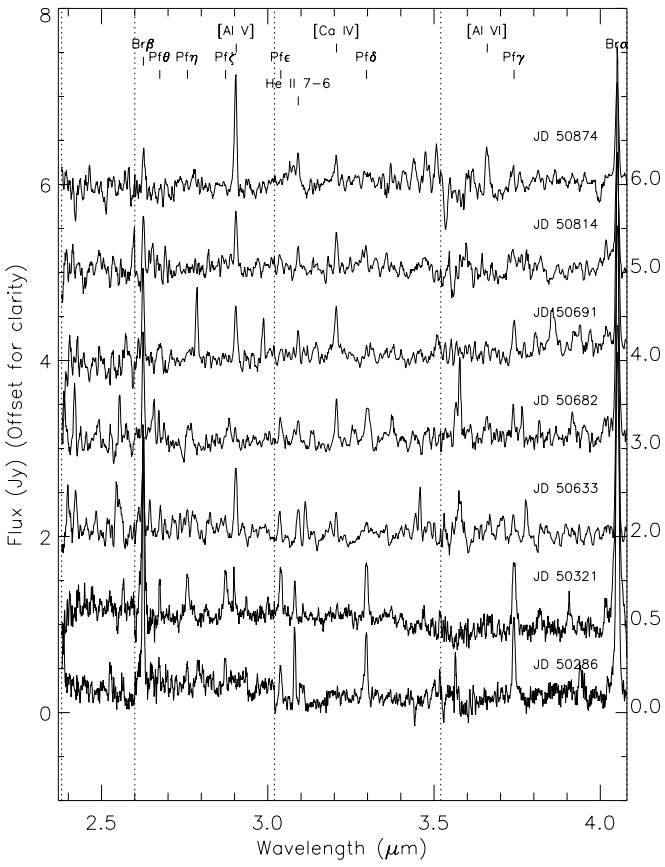

FIG. 2.—Evolution of the 2.4–4 μm spectrum of V723 Cas as seen by *ISO* (SWS) over a $\sim$600 day period. Principal emission lines are identified.

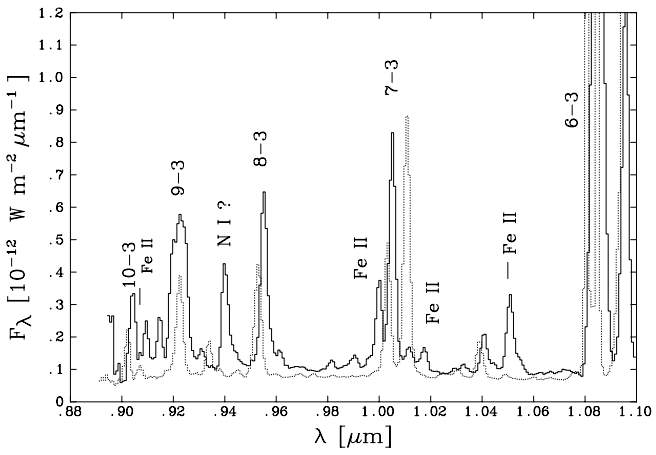

FIG. 3.—*I*-band KPNO (+CRSP) spectrum of V723 Cas. H and He recombination lines are prominent. The data are plotted to reveal details of the weaker lines in the spectra, since [He I] 1.083 μm and the Paγ emission lines are particularly strong. *Thick line*, data obtained on 1996 Jun 11 ($t = 176.3$ days); *thin line*, data obtained on 1997 Nov 15 ($t = 698.1$ days).

Both V723 Cas and V705 Cas 1993 were slow novae. However, we note that V723 Cas, unlike V705 Cas (Salama et al. 1999), continued to show strong IR line emission $\sim$800 days after outburst. In this respect, V723 Cas was similar to, although less extreme than, V1974 Cyg (Salama et al. 1996). A further major difference between V723 Cas and V705 Cas was that the latter formed an optically thick dust shell (Evans et al. 1997; Mason et al. 1998), while the former did not (see § 8 below).

The weighted mean expansion velocity as deduced from the FWHM of the emission lines, after deconvolving the instrumental profiles, is 332 ± 17 km s^{-1}. Where emission lines were resolved, we find that some were double-peaked, hinting at the presence of anisotropies and/or inhomogeneities in the ejecta. The presence of such structure no doubt accounts for the polarization reported by Johnson et al. (1996). There is no evidence for deceleration of the ejecta

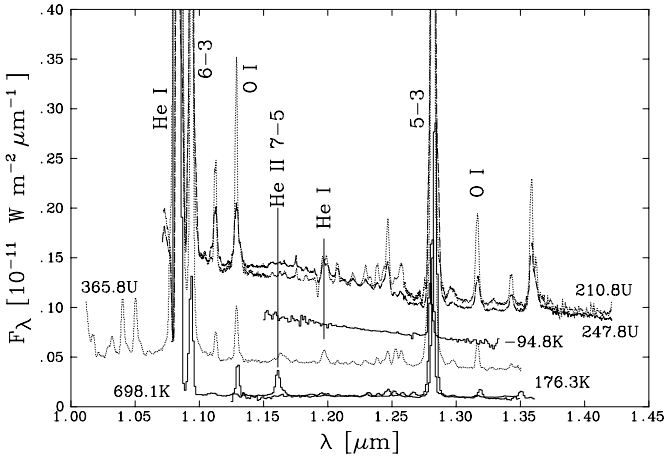

FIG. 4.—*J*-band spectrum of V723 Cas, observed with UKIRT and KPNO (+CRSP). Solid lines are KPNO data, and spectra are labeled by days from maximum (t) and "U/K" for UKIRT/KPNO, respectively. H, He, and O recombination lines are prominent. Note the P Cygni profile in the 1.08 and 1.19 μm He I lines in 1996 August ($t = 247.8$ days). The 1.08 μm line is shown in greater detail in Fig. 11.

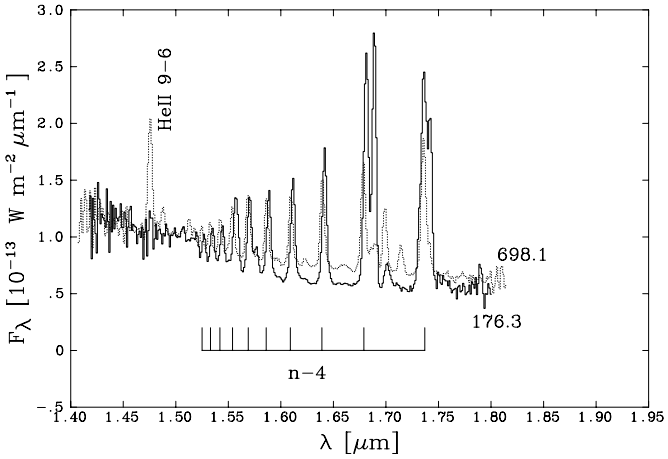

FIG. 5.—*H*-band KPNO (+CRSP) spectra of V723 Cas obtained on 1996 June 11 ($t = 176.3$ days) and 1997 November 15 ($t = 698.1$ days). H recombination lines from the Brackett series ($n \rightarrow 4$) are prominent.

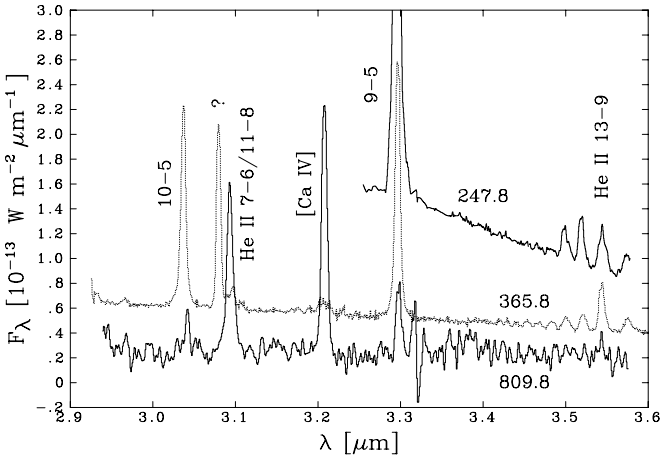

FIG. 7.—Evolution of the *L*-band spectrum of V723 Cas observed with UKIRT from 1996 August to 1998 March. Spectra are labeled by days from maximum.

over the ~900 days of observation. When the ejecta have swept up their own mass of material in the nova environment (be it pre-eruption or interstellar material), significant deceleration of the ejecta occurs. Taking an ejecta mass of $2 \times 10^{-5}\ M_\odot$ (see § 6 below), we place an upper limit of 5.5×10^{-19} g cm^{-3} on any matter in the nova environment prior to eruption.

4. H AND He EMISSION LINES

We use the H I and He II recombination lines in V723 Cas to estimate the reddening, the physical conditions in the ejecta, and the ejected mass.

The time dependence of the flux of a number of H recombination lines, as measured from the ground and from *ISO*, is shown in Figure 9. There is some evidence that the H line fluxes peaked sometime between $t \simeq 200$ and 260 days. The most complete data are for Brα, the first measurement of which was around the peak. A regression through these data indicates that the Brα flux declines as t^{-b}, where the exponent b is close to unity. We suppose therefore that the Brα flux declines with time as (see Fig. 9)

$$f(\mathrm{Br}\alpha) \simeq \frac{(2.57 \pm 0.20) \times 10^{-12}}{t}\ \mathrm{W\ m^{-2}} \quad (t > 250\ \mathrm{days})\ , \tag{1}$$

obtained by forcing a t^{-1} relationship, with t in days. The only H recombination line securely detected longward of Brα was Huα λ12.372, on day 217 with integrated flux $(24.4 \pm 3.4) \times 10^{-16}$ W m^{-2}. It was not detected, to a 3 σ limit of 75×10^{-16} W m^{-2} (45×10^{-16} W m^{-2}), on day 251.9 (612.7).

There were significant changes in the He I 2.058 μm line profile in 1996 (see Figs. 4 and 10), and there are similar changes in Brα (see Fig. 11). Many of the emission lines can be described by double Gaussians, with an overall width associated with expansion velocities around 300 km s^{-1}. At the time of flare A, however, there were significant changes in the line profiles (see Figs. 10 and 11). Both UKIRT and

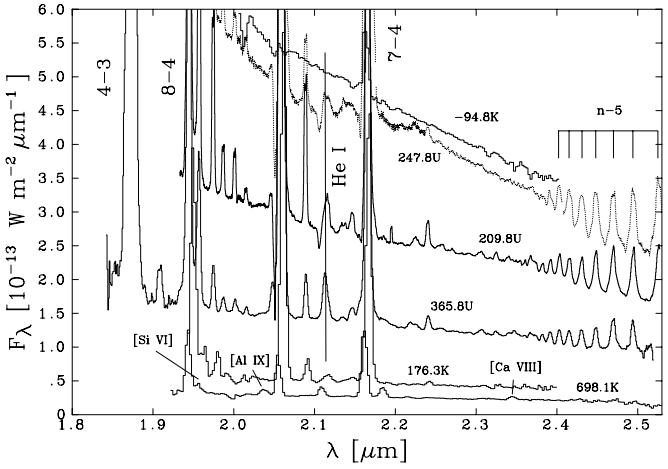

FIG. 6.—*K*-band spectrum of V723 Cas, observed with UKIRT and KPNO (+CRSP). Solid lines are KPNO data, and spectra are labeled by days from maximum (t) and "U/K" for UKIRT/KPNO, respectively. H and He recombination lines are prominent; note the P Cygni profiles in the He I 2.058 and 2.114 μm lines in 1996 July/August ($t = 209.8$ and 247.8 days). Coronal lines [Al IX], [Ca VIII], and [Si VI], present in later spectra, are absent in earlier spectra.

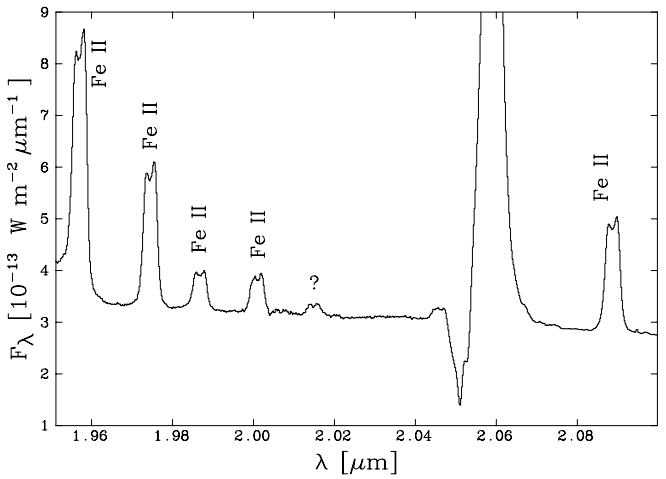

FIG. 8.—Double-peaked line profiles in the UKIRT *K*-band at $t = 209.8$ days.

TABLE 4
OBSERVED H LINE FLUXES (IN 10^{-16} W M^{-2}) IN V723 Cas

t (days)	Pfβ 1.282 μm	Brδ 1.945 μm	Brγ 2.166 μm	Brα 4.052 μm	Huα 12.372 μm
−94.8	19.1 ± 1.0	...	7.9 ± 1.0	...	...
176.2	113 ± 1	...	31.4 ± 1.0	...	...
209.8	...	87.5 ± 23	68.3 ± 12	...	...
210.8	376 ± 12	...	...	...	...
217.0	...	...	...	125 ± 1.0	24.4 ± 3.4
247.8	320 ± 9	...	92.2 ± 4.5	...	...
251.9	...	...	...	92 ± 1.3	<75
365.8	297	47.5 ± 1.0	54.8 ± 1.0	...	...
563.3	...	...	...	40 ± 1.0	...
612.7	...	...	...	49 ± 1.0	<45
621.6	...	...	...	44 ± 1.2	...
689.1	72.5 ± 1.3	7.9 ± 1.0	8.8 ± 1.0	...	...
744.3	...	...	...	28 ± 1.0	...
744.3	...	...	...	29 ± 1.0	...
804.6	...	...	...	23 ± 1.0	...

ISO observations revealed that the H I recombination lines and [Si VI] were double-peaked at times when the He I λ1.083, He I λ2.058, and He I λ2.112 lines showed P Cygni profiles with a terminal velocity of $\approx$1500 km s^{-1} (see Figs. 10 and 11). We note that the P Cygni profiles, present in the UKIRT data on day 210, were not present in the KPNO spectra taken on day 176.3. Iijima et al. (1998) noted the presence of P Cygni profiles in premaximum optical spectra with velocities $\simeq$150 km s^{-1}; the outflow seen in the optical by these authors and in this paper must represent different mass ejection events.

Where the He I lines show P Cygni profiles, there is a distinct emission core at the absorption minimum (see Figs. 4, 10, and 11). Such a combination is sometimes seen in the spectra of colliding wind systems (J. H. Wood 2002, private communication) and suggests that the light curve and spectral behavior in V723 Cas (and presumably of other, similar, novae) is consistent with the interaction of material moving at different velocities.

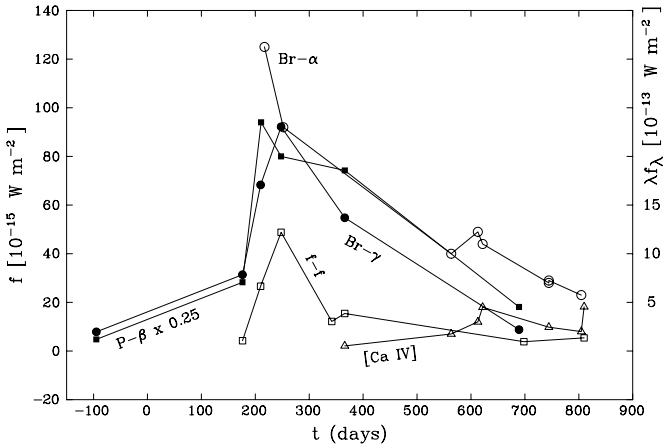

FIG. 9.—Time dependence of the H recombination lines and [Ca IV] fluxes (*left-hand scale*) and free-free emission λf_λ (*right-hand scale*) in V723 Cas. Filled circles, Brγ; open circles, Brα; filled squares, Pfβ; open squares, free-free; and open triangles, [Ca IV]. Lines are included to guide the eye.

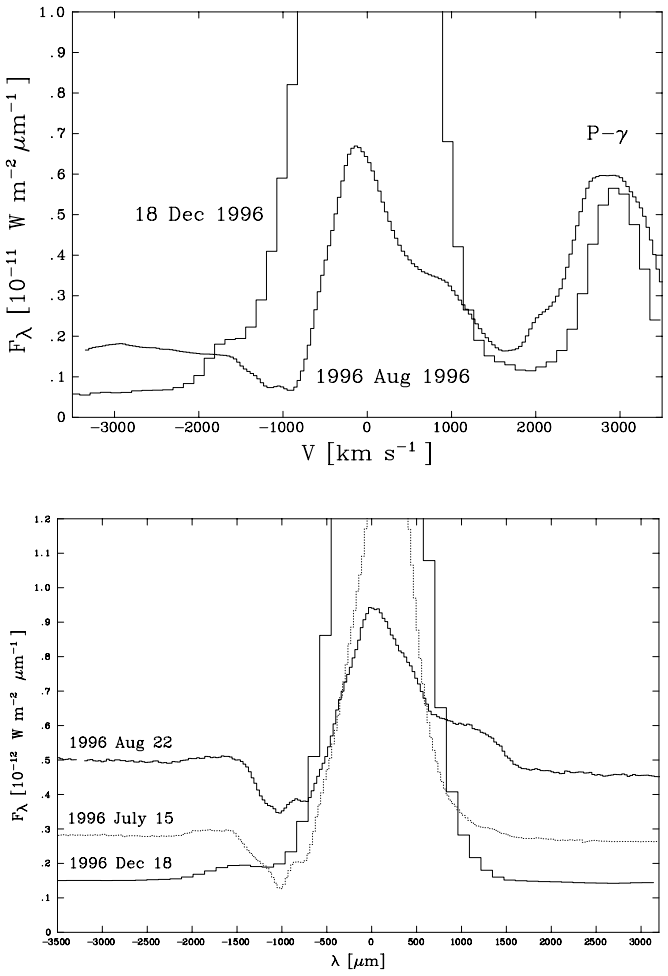

FIG. 10.—Change in the line profile of the He I 1.083 μm (*top*) and 2.058 μm (*bottom*) lines in 1996; horizontal scale is velocity determined from the respective rest wavelengths of the He I lines. Note the P Cygni profile in July and August, indicating outflow velocities of $\sim$1500 km s^{-1}, and the extension redward of the main emission in August.

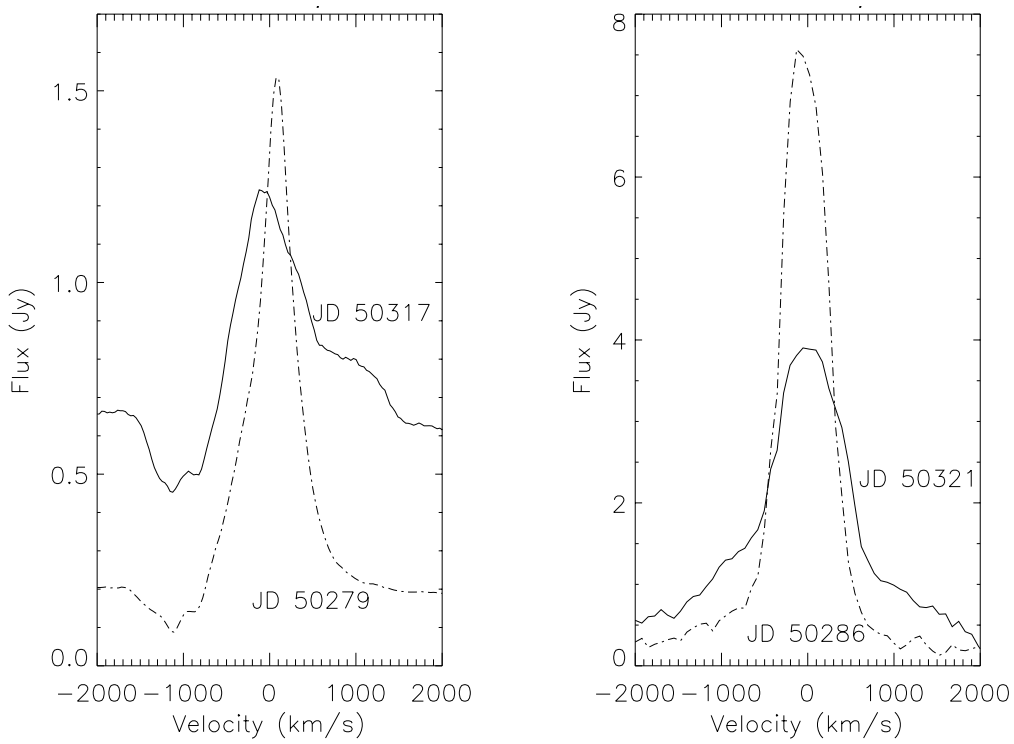

FIG. 11.—Change in line profile for quasi-simultaneous observations taken with UKIRT (*left*) and ISO SWS (*right*) in a He I line and a H I line, respectively, during flare A. The flare in the optical light curve occurred at $t \sim 250$ days; the observations on $\sim$ JD 50,279/86 ($t \simeq 210$ days) were carried out when the light curve was "normal." Note the line profile broadening, indicative of mass ejection at velocities $\sim$1000 km s^{-1}.

4.1. *Electron Density and Temperature*

With the assumptions that the H I recombination lines are (1) optically thin and (2) uncontaminated by other lines (e.g., He II), we can use their flux ratios to determine the physical conditions in the region in which the H I lines originate. We have combined UKIRT data from $t = 247.8$ days with *ISO* data from $t = 252.0$ days and have used the flux ratios Brα/Pfγ, Brγ/H I 22–5, H I 18–5/H I 17–5, and H I 19–5/H I 17–5. Since each ratio is formed from lines with similar wavelength, these ratios are insensitive to the reddening. Using data in Storey & Hummer (1995, hereafter SH95) and assuming that case B (SH95) applies, our data suggest that, in 1996 August, the electron temperature was $T_e \simeq 10^{3.85\pm0.15}$ K ($\simeq$7000 K) and the electron density was $N_e \simeq 10^{8.3\pm0.7}$ cm^{-3} (2×10^8 cm^{-3}) in the region from which the H lines originate. We also note that, at these values of T_e and N_e, He is predominantly singly ionized, with $N(\mathrm{He}^+)/N(\mathrm{He}^0) \simeq 120$ and $N(\mathrm{He}^{2+})/N(\mathrm{He}^+) \simeq 2 \times 10^{-20}$ for a plasma in which collisions dominate; we also expect He^+ to dominate in a photoionized gas in these conditions (Hummer & Seaton 1964).

Thus, while the He I lines (which likely arise from recombination of He^+) may arise in the 7000 K region, it is unlikely that the He II lines (which arise from recombination of He^{2+}) do so. We note, however, that coronal lines are present (see § 7 below), so it seems that there exist both "cool" ($\sim$7000 K) and hot diffuse regions in the ejecta of V723 Cas at this time.

Assuming that the continuum clearly visible in Figs. 3–7 is free-free emission, the electron temperature may, in principle, be obtained independently of reddening from the ratio of H line flux to free-free continuum (Benjamin & Dinerstein 1990). However, the continuum is "too strong" by comparison with the lines: for an isothermal gas at $\sim$7000 K, the ratio $[\lambda f_\lambda]_{\mathrm{cont}}/f(\mathrm{H\ line})$ should be $\sim$9 at Brγ, compared with observed values $\sim$50–100. This suggests that there is an additional source of free-free emission, most likely the coronal gas (Saizar & Ferland 1994).

As noted above, the Brα flux declined approximately as t^{-1} for $t \gtrsim 250$ days, and we have determined the value of N_e for $t \simeq 250$ days. Since the Brα line flux is $\propto N_e^2 V$ (where V is the emitting volume) for constant electron temperature, we take N_e to vary as

$$N_e\ (\mathrm{cm}^{-3}) \simeq 2 \times 10^8 \left[\frac{250}{t\ (\mathrm{days})}\right] \qquad (2)$$

(cf. eq. [1]) to estimate the electron density in the H line region at other times. This dependence of N_e on time clearly does not follow from the expansion of a uniformly filled sphere ($\propto t^{-3}$) or of a thin spherical shell of constant thickness ($\propto t^{-2}$). One possibility is a thin spherical shell, the thickness of which declines as t^{-1}, which might arise as the result of interactions between various components of the ejecta; however, we do not pursue the physics of this situation here.

4.2. *Reddening*

The reddening to V723 Cas has been determined by several authors, using essentially independent methods; these determinations are summarized in Table 5. Gonzalez-Riestra et al. (1996) determined the reddening to be $E(B-V) = 0.6$ on the basis of the strength of the interstellar "2200" extinction feature. This is close to the values obtained [$E(B-V) = 0.54$ and 0.59] by Chochol & Pribulla

TABLE 5
REDDENING OF V723 CAS

$E(B-V)$	Method	Reference
0.60	"2200" extinction feature	1
0.29	Extinction in the field	2
0.45	Na I D lines	3
0.59	Intrinsic nova color at maximum	4
0.54	Intrinsic $B-V$ at $\Delta V = 2$	4
0.55	$B-V$ during "stability stage"	4
0.23 ± 0.16	IR H I recombination lines	5
0.78 ± 0.15	IR H I recombination lines	6

REFERENCES.—(1) Gonzalez-Riestra et al. 1996; (2) Iijima et al. 1998; (3) Munari et al. 1996; (4) Chochol & Pribulla 1997; (5) Rudy et al. 2002; (6) this paper.

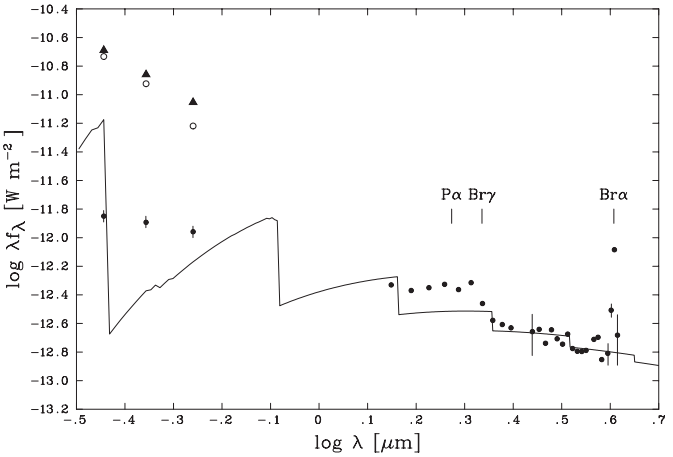

FIG. 12.—Observed narrowband WIRO IR photometry of V723 Cas obtained on 1996 Nov 24.08 UT (day 341.8), with optical *UBV* data from Chochol & Pribulla (1997) from the same epoch (*filled circles*). Error bars are smaller than plotted points unless displayed. Open circles are *UBV* data, dereddened by $E(B-V) = 0.6$. Curve is free-free and free-bound continuum from a gas having typical nova abundances for He and CNO, and with $T_e = 7000$ K and $N_e = 1.4 \times 10^8$ cm^{-3}; the curve is normalized at 5 μm. Filled triangles are combined gas emission and 23,000 K blackbody at *U*, *B*, and *V*, scaled to $D = 4$ kpc. See text for details.

(1997) using color variations and an assumed intrinsic $B-V$, but somewhat larger than the value of $E(B-V) = 0.45$ obtained by Munari et al. on the basis of the strength of interstellar lines and by Iijima et al. (1998) on the basis of the reddening of field stars.

In principle, we can use the IR H I recombination lines to obtain another, independent, determination of the reddening, assuming that the lines are optically thin and that there is negligible contamination by other species. Using our measured IR H I recombination lines, this method yields $E(B-V) \simeq 0.78 \pm 0.15$, somewhat higher that the values determined by the other methods (see Table 5), but consistent with the value obtained by removing the interstellar 2200 feature. This result indicates that the H lines are not particularly optically thick or significantly contaminated by other species. However, the H recombination line method for determining $E(B-V)$ may suffer somewhat from uncertainties in the relative calibrations of the fluxes in the *JHKL* bands and possibly from departure from case B (Venturini et al. 2002). We note the average value of $E(B-V)$ derived from Rudy et al. (2002) is 0.23 ± 0.16, deduced using IR H I recombination lines and assuming case B.

Given the inherent uncertainties in the various methods, we prefer the $E(B-V)$ value implied by the 2200 method, which directly observes the reddening material. We assume here $E(B-V) = 0.6 \pm 0.1$, where the assumed uncertainty is typical of determinations using the 2200 method. The corresponding visual extinction, assuming that the total-to-selective extinction $R = 3.1$ (Cardelli, Clayton, & Mathis 1989), is $A_V = 1.9 \pm 0.3$.

In Figure 12, we combine the spectral energy distribution (SED) as given by the WIRO data for $t = 341.8$ days with *UBV* magnitudes from Chochol & Pribulla (1997), obtained within about 10 days of the WIRO observations; we have assigned a ± 0.1 uncertainty in the optical magnitudes to allow for variations. We assume that the continuum is optically thin free-free and free-bound emission, and we take $T_e = 7000$ K and N_e from equation (2). Our data do not give us any information about the CNO and He abundances in the ejecta of V723 Cas. We therefore assume overabundances typical of novae for these species (see Table 2 of Gehrz et al. 1998) and assume that they are singly ionized. It transpires that the continuum shape, which is included in Figure 12, is insensitive to the assumed composition.

The IR SED seems consistent with optically thin free-free and free-bound emission from 1 to 4 μm with H recombination lines superposed (see Fig. 12). However, the optical data are clearly inconsistent with free-free and free-bound, and dereddening—even by the lower $E(B-V)$ favored by Rudy et al. (2002)—renders the data *inconsistent* with free-free and free-bound emission at optical wavelengths. This suggests that there is an additional source of emission at shorter (optical) wavelengths, possibly the pseudophotosphere that, in a nova with $t_3 \simeq 778$ days (see § 5 below), may still be contributing in the optical/near-IR even after ~340 days.

To explore this possibility, we use the prescription of Bath & Harkness (1989) to estimate the effective temperature of the pseudophotosphere at $t = 341.8$ days and find $\sim 23 \times 10^3$ K. Combining this with a bolometric luminosity $L \simeq 3.3 \times 10^4\ L_\odot$ (see eq. [5] below), we can estimate the *UBV* fluxes from a pseudophotosphere at 4 kpc distance (see § 5) at this time; these are included in Figure 12. Clearly, the 23,000 K blackbody matches well the *UBV* data, dereddended by $E(B-V) = 0.6$, and lends support both to the higher value of reddening and to the continued contribution from the pseudophotosphere to the observed optical emission.

5. DISTANCE

The absolute visual magnitude at maximum is related to the "speed class," the characteristic time for the visual light curve of a nova to decline by 2 or 3 mag (e.g., Payne-Gaposchkin 1957; Dürbeck 1981; Warner 1989, 1995). In view of the erratic nature of the visual light curve (see Fig. 1), the speed class for a nova like V723 Cas is notoriously difficult to determine. Chochol & Pribulla (1997) deduce that t_3, the time for the nova to decay by 3 mag from visual maximum, is 173 ± 5 days on the basis of a linear fit to the light curve over the period JD 2,450,210–2,450,260, which was free of the erratic excursions that occurred at other times (see Fig. 1). On the other hand, when we examine the

light curve over the greater time base of Figure 1, a regression analysis (omitting the flares) gives $t_3 \simeq 778 \pm 50$ days, very much at the low end of nova behavior; the corresponding t_2 (which we use to determine the distance of V723 Cas) is 519 ± 50 days.

To estimate the distance, we need the apparent magnitude at maximum, but this is not easily determined in the case of V723 Cas. We consider that maximum light occurred at $m_{\rm vis} = 8.25 \pm 0.25$ (see Fig. 1), and we use the maximum magnitude–rate of decline (MMRD) relation as calibrated by Della Valle & Livio (1995):

$$M_V = -7.92 - 0.81 \arctan[(1.32 - \log t_2)/0.23] \text{ mag} \quad (3)$$

to find $M_V = -6.78 \pm 0.01$ (note the small uncertainty, which results from the logarithmic dependence of M_V on t_2). The resulting distance D for V723 Cas is 4.2 ± 0.5 kpc with the assumed reddening.

The radio emission from V723 Cas is almost certainly free-free emission and, since the free-free emissivity is $\propto N_e^2 T_e^{-1/2}$, the observed radio emission very likely arises in the cool gas rather than the hot diffuse coronal gas (see § 7 below). The observed expansion velocity of 332 km s^{-1}, as deduced from the H lines, together with the angular diameter at 6 cm (65 mas; Heywood et al. 2003) in 1997 January ($t \simeq 400$ days) can also be used to determine the distance. Assuming that the material responsible for the 6 cm radio emission expanded at the same rate (330 km s^{-1}) as the line emitting material, the implied distance is 2.4 kpc. However, since mass ejection is likely to have commenced prior to t_0, this is a lower limit on D. Even so, it is considerably smaller than the distance deduced above, but similar to that determined by Chochol & Pribulla (1997).

These discrepancies in the distance determinations underline the difficulty of applying the MMRD relation to an object like V723 Cas, and indeed, there arises the question whether or not the MMRD relation applies at all to objects of this kind.

On the basis of the relationship between t_3 and WD mass (e.g., Livio 1992), we infer that the mass of the WD in the V723 Cas system must be very low (see also Iijima et al. 1998), and indeed, lies outside the relationship given by Livio. We therefore make the comparison with HR Del, in which the WD mass is 0.67 $M_\odot$ (Ritter & Kolb 1998), close to the lowest mass on which a nova eruption can occur (Kovetz & Prialnik 1985). Such a WD is likely to be a CO rather than a ONeMg WD, and we expect this to be reflected in the composition of the ejected material. In particular, we note that we do not detect any Ne lines in V723 Cas (cf. Table 8 below), consistent with it not being a "neon nova." If we assume a WD mass of 0.67 $M_\odot$ in V723 Cas, we have, in principle, another means of estimating the nova distance. At maximum, a nova will radiate close to the Eddington luminosity $L_{\rm Edd}$, and we write

$$L \equiv \alpha L_{\rm Edd} , \quad (4)$$

$$\simeq (1.26 \times 10^{31}) \alpha \mu \left(\frac{M_{\rm WD}}{M_\odot} \right) \text{ W} , \quad (5)$$

where α is the bolometric luminosity of the nova in terms of $L_{\rm Edd}$, and μ is the mean atomic mass per electron; with overabundances in the CNO elements as a result of the TNR, we might expect $\mu \simeq 1.5$. At maximum, $B-V$ for V723 Cas was $\simeq 0.21$ (Chochol & Pribulla 1997), indicating effective temperature 7500 K. Using $\mu \simeq 1.5$, we find that

$$M_V \simeq -6.59 - 2.5 \log \alpha . \quad (6)$$

With $m_V \simeq 8.25$ at maximum, we obtain $D = 3.5$ kpc for $\alpha = 1$. We assume $D = 4$ kpc here.

6. EJECTED MASS

We can estimate the ejected mass by following the evolution of Brα (see Figs. 2 and 9), which declines from an integrated flux (reddened) of 12.5×10^{-15} W m^{-2} on day 217 to 2.3×10^{-15} W m^{-2} on day 804. The decline of the integrated flux with time is consistent with t^{-1} (see eq. [1]). At $T_e \simeq 7000$ K and $N_e \simeq 2 \times 10^8$ cm^{-3} (see § 4.1), most of the H is in the form of H^+, while most of the He is in the form of He^+ with negligible He^{2+}. There is therefore negligible contribution to Brα from He II 10–8. Assuming that Brα is optically thin, the mass of H is

$$M_{\rm H}/M_\odot = 20.37 f_{15} \mu N_e^{-1} D_{\rm kpc}^2 , \quad (7)$$

$$\simeq 1.1 \times 10^{-6} \mu D_{\rm kpc}^2 , \quad (8)$$

where f_{15} is the Brα flux in units of 10^{-15} W m^{-2} [dereddened using $E(B-V) = 0.6$] and $D_{\rm kpc}$ is the distance in kiloparsecs. The emissivity of Brα is insensitive to N_e and T_e (SH95) and is included in the numerical constant. The ejected mass $M_{\rm ej}$ is therefore $\sim (1.1 \times 10^{-6}) \mu D_{\rm kpc}^2 \ M_\odot$. With $D = 4$ kpc and $\mu = 1.5$, we have $M_{\rm ej} \simeq 2.6 \times 10^{-5} \ M_\odot$.

Assuming that the continuum in the IR is free-free emission, we can obtain another, independent, estimate of the ejected mass. We see in Figure 9 that the free-free flux rises and falls with the H recombination lines. A similar rise and fall in the free-free flux was seen in the (dustless) V1500 Cyg, in which the decline in the free-free was attributed to the expansion of the optically thin gas (Ennis et al. 1977). If we make this assumption for V723 Cas, we obtain an ejected mass of $\sim (7.3 \times 10^{-6}) \mu D_{\rm kpc}^2 \ M_\odot \simeq 1.7 \times 10^{-4} \ M_\odot$ for $T_e \simeq 7000$ K, higher than that deduced from Brα. This implies that the bulk of the observed free-free emission does not arise in the same region of the ejecta as the H recombination lines.

This discrepancy may be resolved if we suppose, instead, that the free-free emission arises in the coronal gas. In § 7 below, we estimate the temperature in the coronal region to be 3.2×10^5 K; in this case, the ejected mass is $\simeq 4.3 \times 10^{-4}$ $M_\odot$, and the deduced mass is a factor of ~ 10 greater than that obtained using Brα. We have already seen (§ 4.1) that the continuum is too strong by comparison with the H recombination lines. The supposition that the bulk of the free-free emission arises in the coronal zone is therefore in line with our earlier conclusion that the coronal gas is the prime source of the free-free emission in the IR.

These values for the ejected mass are reasonably in line with those found from the radio emission by Heywood et al. (2002), namely 2.5×10^{-4} $M_\odot$, for an electron temperature of 23,000 K and a distance of 2.4 kpc. More detailed calculations (Heywood et al. 2003) show that estimates of ejected mass lie in the range $(0.5–5) \times 10^{-4}$ $M_\odot$ for plausible ranges of electron temperature and distance.

We note here that there is a tendency for the masses of nova ejecta, as determined observationally (e.g., Mason et al. 1996), to be about an order of magnitude greater than theoretical studies of the TNR predict (see Starrfield et al.

2000 for a review). The ejecta mass we have deduced for V723 Cas is in line with this trend.

7. CORONAL AND FINE-STRUCTURE LINE SPECTRUM

"Coronal" emission is well documented in classical novae (e.g., Greenhouse et al. 1990; Gehrz et al. 1998). It was first securely detected ([Ca IV]) in V723 Cas at $t = 365.8$ days; however, [S IX] may have been present at $t = 176.3$ days. Coronal emission was present in all subsequent spectra, to $t = 809.8$ days. The [Al V] 2.904 μm line was first detected at $t = 563.3$ days; [Si X] 1.258 μm was confirmed, and [Si VI] 1.956 μm, [Al IX] 2.036 μm, and [Ca VIII] 2.345 μm were present at $t = 698.1$ days. Table 6 logs the appearance of coronal lines in V723 Cas. We note that the [Al V] λ2.904 μm line was not detected at $t = 612.7$ days, although it was clearly present in the immediately preceding and following observations (see Fig. 2).

The deduced conditions (such as temperature and abundances) in the coronal zone depend on whether one assumes that the "coronal" conditions are a result of photoionization or collisional ionization. This point is discussed by Greenhouse et al. (1990), who find that these two processes may be of comparable importance in novae, although Benjamin & Dinerstein (1990) argue against collisional ionization.

Greenhouse et al. (1990) take "emission lines arising from ground-state fine-structure transitions in species with ionization potential >100 eV" as a working definition of nova coronal lines; we adopt this here. Since the nova pseudophotosphere collapses at constant bolometric luminosity, the effective temperature T_* of the stellar remnant rises as (see Bath & Harkness 1989)

$$T_*(t) \simeq T_0 \exp[0.921(t/t_3)] \, , \qquad (9)$$

where $T_0 = 15{,}280$ K; note that the temperature variation depends on t_3. Eventually, the remnant is hot enough that sufficient photons capable of producing the requisite high ionization are emitted, and the nova enters its "coronal" phase. We suppose that this phase is reached when half the emitted power is in the form of photons with energy $h\nu > \chi_0 = 100$ eV, so that the time $t_{\rm cor}$ at which the nova enters the coronal phase is, from equation (9), given by

$$t_{\rm cor} \simeq (3.34 \pm 1.50) t_3 \, ; \qquad (10)$$

the "error" allows for differences by a factor of 2 in both T_0 and χ_0 from nova to nova. Had we taken half the emitted photons, rather than power, to photoionize the gas, the coefficient in equation (10) would have been 3.77; this difference does not affect the following discussion. This relationship is plotted in Figure 13, together with values of t_3 and $t_{\rm cor}$ taken from Table VIII of Benjamin & Dinerstein (1990). Allowing for the simplicity of our treatment, the agreement is reasonable. Discrepancies above the line can probably be attributed to infrequent spectroscopy of novae so that the onset of the coronal phase is missed, the remainder to the idiosyncrasies of individual novae. Interestingly, even the slow nova HR Del (at $t_3 = 230$ days) conforms with this relationship. This supports the conclusion of Benjamin & Dinerstein (1990) that the "coronal" phase of novae is, in general, the result of photoionization.

However, from equation (10) and with $t_3 = 778$ days (see § 5), we would not expect V723 Cas to enter its coronal phase until ~2600 days after outburst: the effective temperature of

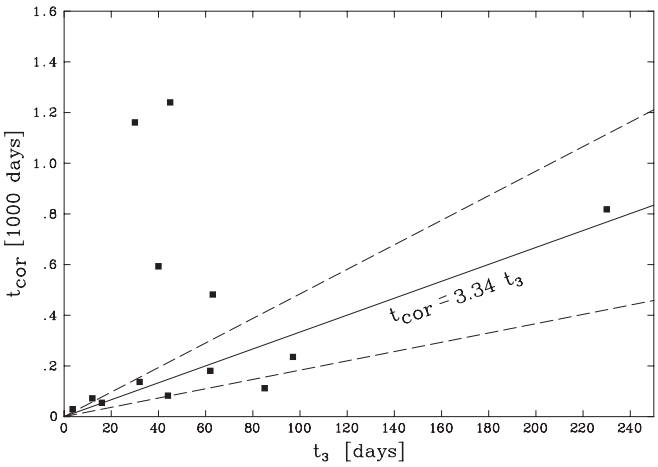

FIG. 13.—Expected time of onset of coronal phase in novae (*solid line*) as a function of t_3, derived from data from Benjamin & Dinerstein (1990). The broken lines allow for differences between novae. See text for details.

TABLE 6
CORONAL LINES OBSERVED IN V723 Cas[a]

t (days)	[S IX] $^3P_2$–$^3P_1$ 1.258 μm $N_c = 7.4(09)$	[Si VI] $^3P_{3/2}$–$^3P_{1/2}$ 1.965 μm $N_c = 1.5\,(09)$	[Al IX] $^3P^\circ_{3/2}$–$^3P^\circ_{1/2}$ 2.036 μm $N_c = 1.5\,(08)$	[Ca VIII] $^3P^3P^\circ_{3/2}$–$^3P^\circ_{1/2}$ 2.345 μm $N_c = 1.5\,(08)$	[Al V] $^2P_{3/2}$–$^2P_{1/2}$ 2.904 μm $N_c = 4.4\,(08)$	[Ca IV] $^2P^2P_{3/2}$–$^2P^\circ_{1/2}$ 3.206 μm $N_c = 1.2\,(08)$	[Al VI] $^3P_2$–$^3P_1$ 3.661 μm $N_c = 4.2\,(08)$
176.3	1.43	...	...	...	...	...	
365.8	...	...	...	...	...	2.11	...
563.3	...	...	...	...	24	7	...
612.7	...	...	...	...	<16	12	...
621.6	...	...	...	...	22	18	...
698.1	2.41	1.06	6.48	3.70	...	...	...
744.3	...	...	...	...	21.4	9.8	...
804.6	...	...	...	...	40	8	12
809.8	...	...	...	...	...	18.2	...

[a] Line fluxes in 10^{-16} W m^{-2}; uncertainties are typically $\pm 1 \times 10^{-16}$ W m^{-2}. Critical densities N_c (in cm^{-3}) at 3.2×10^5 K are written in the form $X(Y) \equiv X \times 10^Y$. Where lines are double, total flux is given. *ISO* fluxes are from SWS01 speed 1 or 2 observations (see Table 2).

the stellar remnant increases so slowly (cf. eq. [9]) that the onset of the coronal phase by photoionization of the ejecta is long delayed. However, in the case of V723 Cas coronal emission was present on day 365.5, possibly from as early as day 173.3, and certainly in all subsequent spectra (see Table 6). It is difficult to see how the stellar remnant is capable of supplying sufficient photons with energy greater than 100 eV at this early time. An alternative explanation for the early onset of the coronal phase in V723 Cas is the presence of ejecta at 330 and at 1500 km s^{-1} and the interaction between the two (cf. § 4). We suggest therefore that collisional ionization is more likely in the case of V723 Cas, and we use the prescription of Greenhouse et al. (1990) to estimate the temperature and abundances in the coronal zone. We stress, however, that the values we deduce should be regarded as pointers rather than definitive values, the determination of which must await detailed modeling.

We use the flux ratios in the [Al VI] and [Al V] lines and, if we interpolate the line flux between $t = 621.6$ and 744.3 days, the [Ca IV] and [Ca VIII] flux ratio. We use collisional strengths from Blaha (1969), Zhang, Graziani, & Pradhau (1994), and Berrington, Saraph, & Tully (1998), and find that the temperature in the coronal zone is $T_{\rm cor} \simeq 10^{5.5\pm0.2} \simeq 3.2 \times 10^5$ K, where the error includes the uncertainty in the fluxes (see § 2.3); we note that this result is insensitive to the reddening, since the lines are at similar wavelengths. This is close to the value found in other novae displaying coronal line emission (Greenhouse et al. 1990; Benjamin & Dinerstein 1990). The critical densities N_c at $T_{\rm cor}$, above which the upper levels of the coronal transitions are collisionally de-excited, are listed in Table 6.

The flux ratios in the coronal lines may also be used to make rough estimates of the abundances of S, Ca, and Al relative to Si using the prescription of Greenhouse et al. (1990) and the elemental ionization fractions from Jain & Narain (1978). The most complete set of data is for day 698.1, for which we find the abundance ratios listed in Table 7. We underline the fact that these values are provisional, since there is inherent uncertainty in taking ionization fractions at the temperature of maximum abundance (Greenhouse et al. 1990). For [Al IX] (which we used to determine Al/Si), maximum abundance occurs at $\sim 10^{5.8}$ K (see Jain & Narain 1978), significantly higher than the $T_{\rm cor}$ assumed here. On the other hand, the other species in Table 6 have maximum abundances at temperatures close to $T_{\rm cor}$, and these values are likely to be more secure.

If we assume that He II lines arise in the coronal region, then the presence of He II (7–6, 11–8 at 3.09 μm), [Al V] 2.904 μm, and [Ca IV] 3.206 μm lines in our *ISO* and UKIRT spectra enables us to make a crude estimate of the Ca/He and Al/He ratios. Making the simplifying assumption that every collisional excitation of Ca^{3+} (Al^{4+}) results in the emission of a [Ca IV] 3.206 μm ([Al V] 2.904 μm) photon (see Benjamin & Dinerstein 1990 for a discussion of how good an approximation this is), the emissivities (in W m^{-3}) in the [Ca IV] and [Al V] lines at 3.2×10^5 K are

$$\epsilon([\mathrm{Ca\ IV}]) \simeq (1.81 \times 10^{-21}) N_e N(\mathrm{Ca}^{3+}) , \quad (11)$$

$$\epsilon([\mathrm{Al\ V}]) \simeq (7.88 \times 10^{-22}) N_e N(\mathrm{Al}^{4+}) , \quad (12)$$

respectively. The emissivity for the He lines is tabulated by SH95, and we have extrapolated their data beyond 10^5 K to $T_{\rm cor}$ using $\epsilon(\mathrm{He\ II}) \propto T^{-1.28}$. At 3.2×10^5 K, He is predominantly doubly ionized (Jain & Narain 1978), and we deduce average abundances of $\sim 7.5 \times 10^{-7}$ (Ca/He) and $\sim 3.9 \times 10^{-6}$ (Al/He) (see Table 7).

We conclude from Table 7 that S/Si, Al/Si, and Ca/Si appear to be significantly enhanced over their solar values, while Al/He and Ca/He are significantly below solar. The latter is a natural consequence of the TNR on a low-mass WD, which results in overabundance of He relative to Al and Ca. This is because, for a 0.67 $M_\odot$ WD, the abundances of the latter two are unaffected by the TNR and should remain close to their pre-TNR values. However, the apparent overabundance of S and Ca relative to Si is problematic. For a TNR on a 0.67 $M_\odot$ WD, the peak temperature is $\sim 1.5 \times 10^8$ K (e.g., Starrfield et al. 1998). While such temperatures may lead to the overabundance of Al observed, it is difficult to see how S and Ca are enriched in the case of V723 Cas; the production of these elements requires a TNR on a massive WD (Starrfield et al. 1998). Perhaps the likely evolved nature of the secondary (see § 1) may be relevant in this respect, and that enhanced S and Ca originate in the secondary.

We did not detect the [O IV] $^2P_{1/2}$–$^2P_{3/2}$ line at 25.89 μm, although it is present in the *ISO* spectra of many other novae, both in eruption and several decades after outburst (Salama et al. 1996, 1998, 1999; Lyke et al. 2001). In the case of V723 Cas, possibly the electron density in its coronal region was too high for the appearance of [O IV]. Limits on the peak and integrated fluxes for selected fine-structure lines, together with critical densities at $T_{\rm cor}$, are given in Table 8 for the *ISO* observation of 1998 March 1. The absence of Ne lines is no doubt connected with the fact that V723 Cas was not a neon nova (see § 5).

Greenhouse et al. (1990) have predicted that [C II] $^2P_{1/2}$–$^2P_{3/2}$ at 157 μm should be strong in coronal line novae. This line is present in the LWS spectrum of V723 Cas, with a mean flux of $\simeq (4.3 \pm 0.7) \times 10^{-16}$ W m^{-2} and a FWHM of 1200 km s^{-1} (the line is unresolved). However, the [C II] line is also present in the background observation (see § 2.1) with essentially the same line flux [$(4.2 \pm 1.6) \times 10^{-16}$ W m^{-2})] and FWHM (1150 km s^{-1}). We conclude therefore that the observed [C II] emission line arises entirely in the interstellar medium and is not present in the spectrum of V723 Cas; however, the critical density for this transition is extremely low (see Table 8).

The critical densities for the coronal lines in Table 6 are all close to the electron densities in the H recombination region, as determined from equation (2). It is clear that there were two distinct regions in the ejecta of V723 Cas: a "cool" region ($\sim$7000 K), responsible for the H I, He I, and some of the near-IR free-free emission, and a "hot" region ($\sim 3.2 \times 10^5$ K) in which the coronal line emission, the He II lines, and the remainder of the near-IR free-free emission originated (Greenhouse et al. 1990).

TABLE 7
ELEMENTAL ABUNDANCES IN THE CORONAL ZONE OF V723 Cas

Ratio	X/Y	$[X/Y]/[X/Y]_\odot$
S/Si	2.2	4.1
Al/Si	1.5	17.1
Ca/Si	1.6	25.3
Al/He	3.9×10^{-6}	0.13
Ca/He	7.5×10^{-7}	0.03

TABLE 8
THREE SIGMA UPPER LIMITS ON FLUXES IN SELECTED CORONAL AND FINE-STRUCTURE LINES ON JD 2,450,874 (t = 804.6 days)

λ (μm)	Ion	Transition	N_c[a] (cm^{-3})	Peak Flux (Jy)	Flux Limit (10^{-15} W m^{-2})
4.487	[Mg IV]	$^2P_{1/2}$–$^2P_{3/2}$	1.5 (08)	2.1	2.7
7.652	[Ne VI]	$^2P_{3/2}$–$^2P_{1/2}$	6.1 (06)	1.8	1.5
12.813	[Ne II]	$^2P_{1/2}$–$^2P_{3/2}$	7.4 (06)	4.5	2.1
14.321	[Ne V]	$^3P_2$–$^3P_1$	1.5 (06)	2.7	1.2
15.555	[Ne III]	$^3P_1$–$^3P_2$	3.4 (06)	6.0	2.4
24.317	[Ne V]	$^3P_1$–$^3P_0$	3.3 (05)	2.4	0.6
25.890	[O IV]	$^2P_{3/2}$–$^2P_{1/2}$	8.5 (04)	2.4	0.6
57.317	[N III]	$^2P_{3/2}$–$^2P_{1/2}$	5.8 (03)	19.7	10
63.184	[O I]	$^3P_1$–$^3P_2$	1.8 (04)	15.9	8
88.356	[O III]	$^3P_1$–$^3P_0$	3.2 (03)	39.1	20
157.741	[C II]	$^2P_{3/2}$–$^2P_{1/2}$	2.3 (02)	...	<10

[a] Critical densities N_c at 3.2×10^5 K are written in the form $X(Y) \equiv X \times 10^Y$.

8. DUST FORMATION

Geisel, Kleinmann, & Low (1970) noted an apparent excess at 5 and 10 μm in the very slow nova HR Del some 3 yr after outburst, and they speculated that this might have been due to emission by dust at ~300 K. However, analysis of *IRAS* observations of HR Del (Dinerstein 1986; Callus et al. 1987; Harrison & Gehrz 1988) suggested that the far-IR emission seen by *IRAS* in 1983 at least was due to fine-structure line emission.

In the case of V723 Cas, we can be confident that little or no dust was produced. There is no evidence for continuum dust emission in the SWS wavelength range (2–40 μm) in any of our observations. We can also rule out emission in the "hydrocarbon" features sometimes seen in novae (Greenhouse et al. 1990; Evans et al. 1997). We can give 3 σ upper limits on any continuum emission of 0.3, 1.2, 0.8, and 2.1 Jy in the wavelength ranges 2.38–4, 4–5.3, 5.3–12, and 12–30 μm, respectively. These limits allow for the presence of only very small amounts of hot dust (temperature $T_d \sim 1000$ K) and/or cooler dust ($T_d \sim 300$ K). Taking the emissivity of carbon in Evans et al. (1997) and $D = 4$ kpc, the 3 σ limits on the dust mass are $2.4 \times 10^{-9}\ M_\odot$ (hot dust) and $6.0 \times 10^{-9}\ M_\odot$ (cool dust). The corresponding limits on the dust-to-gas ratios (by mass) are $\sim 10^{-4}$ for the 7000 K region and $\sim 10^{-5}$ for the coronal region (see Table 9).

We also note that V723 Cas was observed with *HST*/NICMOS by Krautter et al. (2002), who did not detect any extended emission in medium-band filters; this nondetection is consistent with the apparent absence of dust formation as seen by *ISO*.

The dust-to-gas ratio in V723 Cas was low; by contrast, $M_d/M_{\rm gas} \gtrsim (8.4\text{–}24.\ 8) \times 10^{-4}$ for the hot dust in nova V1425 Aql (Mason et al. 1996), which was not a particularly spectacular dust producer. Clearly, conditions in the ejecta of V723 Cas did not favor the nucleation of dust (as was also the case for HR Del, a nova similar in many other ways to V723 Cas). Whether this is connected with elemental abundances, or with the fact that V723 Cas was a "coronal" nova, or with its speed class, or some other factor, remains to be determined.

TABLE 9
THREE SIGMA LIMITS ON DUST-TO-GAS RATIO IN V723 Cas

T_d (K)	Brα	Free-Free
1000	9.4×10^{-5}	5.7×10^{-6}
300	2.3×10^{-4}	1.4×10^{-5}

9. CONCLUSIONS

We have obtained IR spectroscopy of V723 Cas over the wavelength range 1–200 μm, over a ~800 day period. The IR spectrum was dominated by H and He recombination lines and, at later times, by coronal emission. We find evidence for a two-phase ejecta, with (1) a cool ($\simeq$7000 K), dense component in which the H and He^+ recombination lines originate and with mass $2.6 \times 10^{-5}\ M_\odot$, and (2) a hot ($\sim 3.2 \times 10^5$ K), diffuse component responsible for coronal emission and He^{++} recombination lines and having mass $4.3 \times 10^{-4}\ M_\odot$. The latter is broadly in line with other observational determinations of ejected nova masses and is *uncomfortably* high compared with that expected by TNR theory (Gehrz et al. 1998; Starrfield et al. 2000).

The coronal lines allow us to estimate the relative abundances of S, Ca, Al, Si, and He in the coronal zone. The implied overabundance of Al relative to Si is not unexpected, but that of S and Ca is; this is most likely due to the limitations of the method used to estimate the abundances, but may also suggest (as does the orbital period of the V723 Cas system) that the secondary may be evolved, so that some of the elemental enhancement may predate the TNR. The V723 Cas system therefore seems to be a binary system consisting of an evolved secondary with a compact component consisting of a low-mass CO WD; possibly this combination accounts for some of the somewhat anomalous (in nova terms) properties of this object.

There was no evidence of dust emission at any wavelength, leading us to conclude that the dust-to-gas ratio in V723 Cas was significantly low, lower even than in novae showing only a modest ability to form dust.

The properties of V723 Cas are summarized in Table 10.

TABLE 10
PROPERTIES OF V723 Cas

Property	Value
Discovery date	1995 Aug 24.5 (=JD 2,449,954.0)
Assumed t_0	JD 2,450,069.7 ± 0.2
$[m_{vis}]_{max}$	8.25 ± 0.25
t_2 (days)	519 ± 50
t_3 (days)	778 ± 50
$E(B-V)$	0.6 ± 0.1
A_V	1.9
Distance (kpc)	4.0
Ejected mass ($M_\odot$)	2.6×10^{-5} (Brα)
Ejected mass ($M_\odot$)	4.3×10^{-4} (IR free-free emission)
Ejected mass ($M_\odot$)	$(0.5–5) \times 10^{-4}$ (radio free-free emission)[a]
Dust mass ($M_\odot$)	$\lesssim 2.4 \times 10^{-9}$ ($T_d = 1000$ K)
	$\lesssim 2.4 \times 10^{-7}$ ($T_d = 300$ K)
Orbital Period	0.69325 ± 0.00018 days[b]

[a] From Heywood et al. 2003.
[b] From Chochol et al. 2000.

We thank the referee, Rick Rudy, for his constructive comments on an earlier version of this paper. A. E. acknowledges helpful discussions on the radio emission of V723 Cas with Tim O'Brien and Ian Heywood. The *Infrared Space Observatory* (*ISO*) is an ESA project with instruments funded by ESA Member States (especially the PI countries France, Germany, the Netherlands, and the United Kingdom) and with the participation of ISAS and NASA. The *ISO* Spectral Analysis Package (ISAP) is a joint development by the LWS and SWS Instrument Teams and Data Centers. OSIA is a joint development of the SWS consortium. Contributing institutes are SRON, MPE, KUL, and the ESA Astrophysics Division. R. D. G., C. E. W. and J. E. L. were supported by NASA; C. E. W. also acknowledges support from the National Science Foundation (NSF). S. G. S. was partially supported by NASA and by NSF grants to A. S. U. T. R. G. and T. H. L. are supported by the Gemini Observatory, which is operated by the Association of Universities for Research in Astronomy, Inc., on behalf of the international Gemini partnership of Argentina, Australia, Brazil, Canada, Chile, the United Kingdom, and the United States of America. The United Kingdom Infrared Telescope is operated by the Joint Astronomy Centre on behalf of the UK Particle Physics and Astronomy Research Council. We wish to thank T. Nagata for his assistance with the WIRO observations.

REFERENCES

Bath, G. T., & Harkness, R. P. 1989, in Classical Novae, ed. M. F. Bode & A. Evans (Chichester, NY: Wiley), 61
Benjamin, R. A., & Dinerstein, H. L. 1990, AJ, 100, 1588
Berrington, K. A., Saraph, H. E., & Tully, J. A. 1998, A&AS, 129, 161
Blaha, M. 1969, A&A, 1, 42
Bode, M. F., & Evans, A. 1989, in Classical Novae, ed. M. F. Bode & A. Evans (Chichester, NY: Wiley), 163
Callus, C. M., Evans, A., Albinson, J. S., Mitchell, R. M., Bode, M. F., Jameson, R. F., King, A. R., & Sherrington, M. 1987, MNRAS, 229, 539
Cardelli, J. A., Clayton, G. C., & Mathis, J. S. 1989, ApJ, 345, 245
Chochol, D., O'Brien, T. J., & Bode, M. F. 1999, Proc. Warner Symp., Cataclysmic Variables: A 60th Birthday Symposium in Honor of Brian Warner, ed. P. Charles, E. Kuulkers, & T. Shahbaz (Oxford: Elsevier)
Chochol, D., & Pribulla, T. 1997, Contrib. Astron. Obs. Skalnaté Pleso, 27, 53
Chochol, D., Pribulla, T., Shemmer, O., Retter, A., Shugarov, S. Y., Goranskij, V. P., & Katysheva, N. A. 2000, IAU Circ., No. 7351
Clegg, P. E., et al. 1996, A&A, 315, L38
de Graauw, Th., et al. 1996, A&A, 315, L49
Della Valle, M., & Livio, M. 1995, ApJ, 452, 704
Dinerstein, H. L. 1986, AJ, 92, 1381
Drechsel, H., Rahe, J., Dürbeck, H. W., Kohoutek, H. W., & Seitter, W. C. 1977, A&AS, 30, 323
Dürbeck, H. W. 1981, PASP, 93, 165
Ennis, D., Beckwith, S., Gatley, I., Matthews, K., Becklin, E. E., Elias, J., Neugebauer, G., & Willner, S. P. 1977, ApJ, 214, 478
Evans, A., Geballe, T. R., Rawlings, J. M. C., Eyres, S. P. S., & Davies, J. K. 1997, MNRAS, 292, 192
Eyres, S. P. S., Davis, R. J., Watson, S. K., & Bode, M. F. 1997, IAU Circ., No. 6594
Gehrz, R. D. 1988, ARA&A, 26, 377
———. 1990, in IAU Colloq. 122, Physics of Classical Novae, ed. R. Viotti & A. Cassatella (New York: Springer), 138
Gehrz, R. D., Truran, J. W., Williams, R. E., & Starrfield, S. 1998, PASP, 110, 3
Geisel, S. L., Kleinmann, D. E., & Low, F. J. 1970, ApJ, 161, L101
Gonzalez-Riestra, R., Shore, S. N., Starrfield, S., & Krautter, J. 1996, IAU Circ., No. 6295
Greenhouse, M. A., Grasdalen, G. L., Woodward, C. E., Benson, J., Gehrz, R. D., Rosenthal, E., & Skrutskie, M. F. 1990, ApJ, 352, 307
Gry, C., et al. 2002, The ISO Handbook, Vol. 3, The Long Wavelength Spectrometer, Version 2.0 (ESA SP-1262, SAI-99-077/Dc) (Noordwijk: ESA)
Harrison, T. E., & Gehrz, R. D. 1988, AJ, 96, 1001
Heywood, I., O'Brien, T. J., Eyres, S. P. S., Bode, M. F., & Davis, R. J. 2002, in AIP Conf. Proc. 637, Classical Nova Explosions, ed. M. Hernanz & J. José (Woodbury, NY: AIP), 242
———. 2003, MNRAS, submitted
Hirosawa, K., & Yamamoto, M. 1995, IAU Circ., No. 6213
Hjellming, R. M., Wade, C. M., Vandenberg, N. R., & Newell, R. T. 1979, AJ, 84, 1619
Hummer, D. G., & Seaton, M. J. 1964, MNRAS, 127, 217
Iijima, T., & Rosino, L. 1995, IAU Circ., No. 6214
Iijima, T., Rosino, L., & Della Valle, M. 1998, A&A, 338, 1006
Jain, N. K., & Narain, U. 1978, A&AS, 31, 1
Johnson, J. J., Bjorkman, K. S., & Babler, B. L. 1996, IAU Circ., No. 6283
Joyce, R. R. 1992, in ASP Conf. Ser. 23, Astronomical CCD Observations and Reduction Techniques, ed. S. B. Howell (San Francisco: ASP), 258
Joyce, R. R., Fowler, A. M., & Heim, G. B. 1994, Proc. SPIE, 2198, 725
Kamath, U. S., & Ashok, N. M. 1999, A&AS, 136, 107
Kessler, M., et al. 1996, A&A, 315, L27
Kobayashi, N., Nagata, T., Takeuchi, T., Takami, H., & Sato, S. 1996, in ASP Conf. Ser. 97, Polarimetry of the Interstellar Medium, ed. W. G. Roberge & D. C. B. Whittet (San Francisco: ASP), 106
Kovetz, A., & Prialnik, D. 1985, ApJ, 291, 812
Krautter, J., et al. 2002, AJ, 124, 2888
Kurucz, R. L. 1979, ApJS, 40, 1
Leech, K., et al. 2002, The ISO Handbook, Vol. 5, The Short Wavelength Spectrometer, Version 2.0 (ESA SP-1262, SAI/2000-008/Dc) (Noordwijk: ESA)
Livio, M. 1992, ApJ, 393, 516
Lyke, J. E., et al. 2001, AJ, 122, 3305
———. 2003, AJ, 126, 993
Mason, C. G., Gehrz, R. D., Woodward, C. E., Smilowitz, J. B., Greenhouse, M. A., Hayward, T. L., & Houck, J. R. 1996, ApJ, 470, 577
Mason, C. G., Gehrz, R. D., Woodward, C. E., Smilowitz, J. B., Hayward, T. L., & Houck, J. R. 1998, ApJ, 494, 783
Munari U., et al. 1996, A&A, 315, 166
Ohsima, O., Akazawa, H., & Ohkura, N. 1996, Inf. Bull. Variable Stars, No. 4295
Payne-Gaposchkin, C. 1957, The Galactic Novae (Amsterdam: North-Holland)
Ritter, H., & Kolb, U. 1998, A&AS, 129, 83
Rudy, R. J., Lynch, D. K., Mazuk, S., Venturini, C. C., Puetter, R. C., & Perry, R. B. 2003, BAAS, 34, 1162
Rudy, R. J., Venturini, C. C., Lynch, D. K., Mazuk, S., & Puetter, R. C. 2002, ApJ, 573, 794
Saizar, P., & Ferland, G. J. 1994, ApJ, 425, 755
Salama, A., et al. 1998, in *ISO*'s View of Stellar Evolution, ed. L. B. F. M. Waters, C. Waelkens, K. A. van der Hucht, & P. A. Zaal (Dordrecht: Kluwer), 227
Salama, A., Evans, A., Eyres, S. P. S., Leech, K., Barr, P., & Kessler, M. F. 1996, A&A, 315, L209
Salama, A., Eyres, S. P. S., Evans, A., Geballe, T. R., & Rawlings, J. M. C. 1999, MNRAS, 304, L20

Starrfield, S., Truran, J. W., & Sparks, W. M. 2000, NewA Rev., 44, 81
Starrfield, S., Truran, J. W., Wiescher, M. C., & Sparks, W. M. 1998, MNRAS, 296, 502
Storey, P. J., & Hummer, D. G. 1995, MNRAS, 272, 41 (SH95)
Tokunaga, A. T. 2000, in Allen's Astrophysical Quantities, ed A. N. Cox (4th ed.; New York: Springer)
Venturini, C. C., Rudy, R. J., Lynch, D. K., Mazuk, S., & Puetter, R. C. 2002, AJ, 124, 3009
Warner, B. 1989, in Classical Novae, ed. M. F. Bode & A. Evans (New York: Wiley), 1
———. 1995, Cataclysmic Variable Stars (Cambridge: Cambridge Univ. Press)
Williams, P. M., Longmore, A. J., & Geballe, T. R. 1996, MNRAS, 279, 804
Zhang, H. L., Graziani, M., & Pradhau, A. K. 1994, A&A, 283, 319